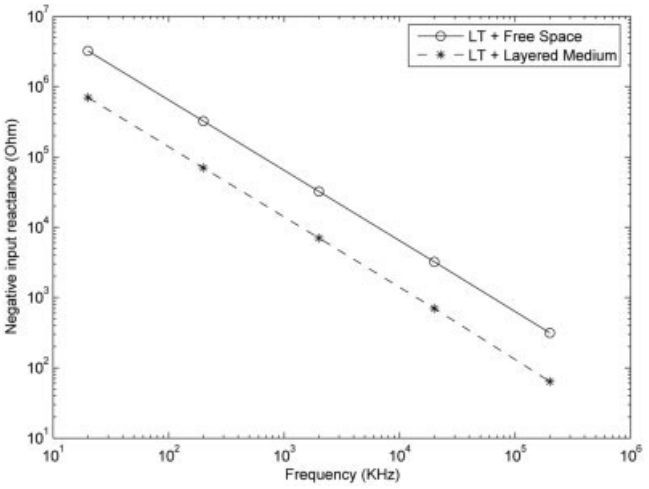

Figure 8 Negative input reactance of the capacitor, $\varepsilon_{r2} = 6.0$

tree results are more stable than RWG ones. As the last example, a rectangular parallel capacitor, shown in Figure 7, is presented. The negative input reactance is plotted in Figure 8, compared with the one from free space. It is demonstrated again that loop-tree basis maintains the low- frequency scale invariance property very well.

6. CONCLUSION

Numerical analysis of electrically small structures embed- ded in a layered medium is presented in this letter. By decomposing the current into the divergence-free part and the nondivergence-free part according to the property of the current in the low frequency regime, we can capture both capacitance and inductance physics, which are of the same importance in circuit physics. Mathematically, loop-tree decomposition combined with frequency normalization makes the matrix stable. The matrix-friendly formulation of LMGF is implemented for its elegant form, and frequency scaling property of the matrix element with this kernel is analyzed before frequency normalization. The con- nection matrix is applied to make the final system amenable to iterative solvers.

ACKNOWLEDGMENTS

This work was supported by 111 Project under Contract No. B07046, SRC Customization Project 1401 and HKU UGC grant.

REFERENCES

1. W.C. Chew, Waves and fields in inhomogeneous media, Van Nostrand Reinhold, Reprinted by IEEE Press, New York, NY, (1995).
2. K.A. Michalski and D. Zheng, Electromagnetic scattering and radiation by surfaces of arbitrary shape in layered media, part I: Theory, IEEE Trans Antennas Propag 38 (1990), 335–344.
3. W.C. Chew, J.S. Zhao, and T.J. Cui, The layered medium Green's function—a new look, Microwave Opt Technol Lett 31 (2001), 252–255.
4. W.C. Chew, J.L. Xiong, and M.A. Saville, A matrix-friendly formulation of layered medium Green's function, IEEE Antennas Wireless Propag Lett 5 (2006), 490–494.
5. J.R. Mautz and R.F. Harrington, An E-field solution for a conducting surface small or comparable to the wavelength, IEEE Trans Antennas Propag 32 (1984), 330–339.
6. E. Arvas, R.F. Harrington, and J.R. Mautz, Radiation and scattering from electrically small conducting bodies of arbitrary shape, IEEE Trans Antennas Propag 34 (1986), 66–77.
7. J.S. Zhao and W.C. Chew, Integral equation solution of maxwell's equations from zero frequency to microwave frequencies, IEEE Trans Antennas Propag 48 (2000), 1635–1645.
8. S.Y. Chen, W.C. Chew, J.M. Song, and J.S. Zhao, Analysis of low frequency scattering from penetrable scatterers, IEEE Trans Geosci Remote Sensing 39 (2001), 726–735.
9. Y.H. Chu and W.C. Chew, Large-scale computation for electrically small structures using surface-integral equation method, Microwave Opt Technol Lett 47 (2005), 525–530.
10. E. Simsek, Q.H. Liu, and B. Wei, Singularity subtraction for evaluation of Green's functions for multilayer media, IEEE Trans Microwave Theory Tech 54 (2006), 216–225.

ANALYSIS OF OPTICAL AND TERAHERTZ MULTILAYER SYSTEMS USING MICROWAVE AND FEEDBACK THOERY

Dong-Joon Lee and John F. Whitaker
Center for Ultrafast Optical Science and Department of Electrical Engineering and Computer Science, University of Michigan, Ann Arbor, MI 48109-2099; Corresponding author: dongjl@umich.edu

Received 2 September 2008

ABSTRACT: *The principles of microwave and feedback theory are independently applied to the analysis of both optical and terahertz-regime multilayer systems. An analogy between the two approaches is drawn, and useful recursion relations, along with a signal-flow approach, are presented for both reflection and transmission cases. These relations, in terms of S-parameters, allow an exact analytical solution for even arbitrary, active, stratified structures, not only for any wavelength in the radio-frequency spectrum, but also for optical wavelengths. This approach also provides a bridge between the microwave and optical bands and leads to beneficial design solutions for intermediate bands such as the THz regime. Comparisons with conventional methodologies are provided using practical multilayer simulations. In addition, graphical design techniques from microwave theory are used along with examples for efficient design and understanding.* © 2009 Wiley Periodicals, Inc. Microwave Opt Technol Lett 51: 1308–1312, 2009; Published online in Wiley InterScience (www.interscience.wiley.com). DOI 10.1002/mop.24301

Key words: *inhomogeneous media; optical feedback; optical films; optical filters; photonics; signal flow graphs*

1. INTRODUCTION

The matrix approach has been the most widely used method to analyze optical multilayers because of its mathematical convenience for quantifying cascaded structures. Transmission-line theory in microwave systems with cascaded elements, on the other hand, has widely used nonmatrix methods. These microwave approaches have been difficult to extend to optical applications due to the reliance in optics on the concept of refractive index. However, analogies between optical thin films and electrical transmission lines have been considered because of the similarity between the transmission impedance and refractive index of a layer [1]. This analogy enables optical multilayers to take advantage of conventional microwave circuit theory for stratified, planar-structure analysis [2–4].

One alternative to the matrix approach is called the signal-flow-graph technique, introduced by Mason [5] and widely used in the analysis of microwave circuits [6]. It has also found only limited use in optical engineering [7, 8].

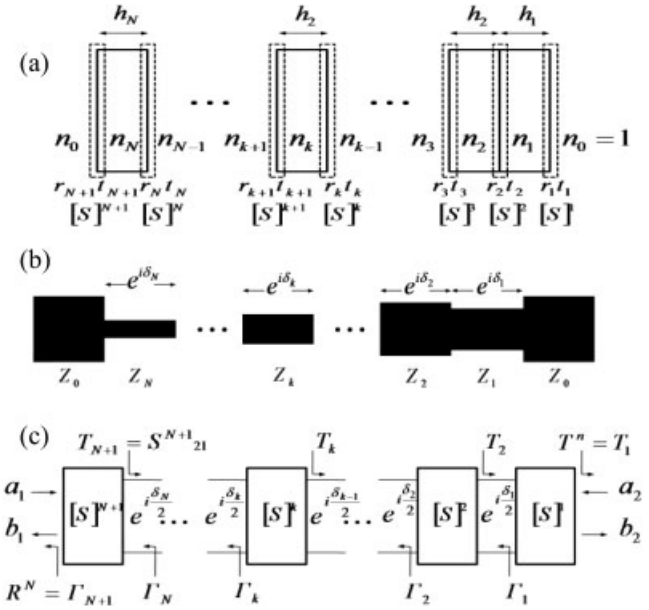

Figure 1 Multiple Fabry-Perot etalon: (a) optical model, (b) transmission-line model (where $n_2 < n_1 < n_k < n_N$), and (c) equivalent network diagram

In this article, the inconvenience of utilizing impedance- based and signal-flow analyses for optical feedback is overcome by exploring the recursive relations of reflection and transmission of optical dielectric multilayers from the microwave perspective. An equivalent subsystem in a recursive format overcomes mathematical complexity and allows for the development of a simple programming algorithm. Since this approach manipulates each layer step by step and naturally provides the reflection and transmission for every layer, it enhances the understanding of the power flow though the layers.

Here, the analytical expressions for double layers are explored through the signal-flow approach and reorganized to the recursive form with an equivalent-flow graph. We also provide examples of an analysis on a typical dielectric thin- film reflector through the recursion formula, and include a graphical interpretation using the Smith chart. Furthermore, the latter illustrates the reflection transition through each layer and yields excellent design insight. Comparisons with examples of practical designs in both the optical and THz bands are presented.

2. MICROWAVE APPRAOCH

An arbitrary, optical, dielectric multilayer is shown in Figure 1(a). For the sake of simplicity, normal-incidence light from free space to a lossless medium is considered.

Since the inhomogeneous discontinuity at each boundary, *k,* causes a partial field reflection (the Fresnel coefficient, r_k) based on refractive-index (n) differences, the two boundaries of a k-th layer create a unique phase-delay ($\delta_\kappa = 4\pi n_k h_k/\lambda$) loop. This delay is determined by the refractive index (n_k) and the thickness (h_k) of the k-th layer, as well as the wavelength (λ). Such an optical-feedback system can be remodeled as a microwave transmission line in terms of the same phase delay and discontinuity. Each discontinuity can be expressed as a scattering matrix [Eq. (1), with S following the standard notation, the k values indicating the boundaries, and Z being impedance], with the round-trip phase delay for each of the k layers given in Eq. (2).

$$[S]^k = \begin{bmatrix} S_{11}^k & S_{12}^k \\ S_{21}^k & S_{22}^k \end{bmatrix} = \begin{bmatrix} r_k & t_k \\ t_k & -r_k \end{bmatrix}, \; k = 1,2, \ldots, n+1 \tag{1}$$

$$\text{where} \quad r_k = \frac{n_k - n_{k-1}}{n_k + n_{k-1}} = \frac{Z_k - Z_{k-1}}{Z_k + Z_{k-1}}, \; t_k = \sqrt{1 - r_k^2}$$

$$\delta_1 = \frac{4\pi n_1 h_1}{\lambda}, \; \delta_2 = \frac{4\pi n_2 h_2}{\lambda}, \ldots, \; \delta_N = \frac{4\pi n_N h_N}{\lambda} \tag{2}$$

At the k-th boundary, the reflectance is $R_k = r_k^2$, thus $T_k = t_k^2$ is the remaining transmittance for a lossless medium. (The conventional definition, $t_k = 2n_k/(n_k - n_{k-1})$ is the Fresnel electric- field transmission coefficient. Here, t_k is a transmission field coefficient to satisfy the $R_k + T_k = 1$ relation.) Z_0 is the characteristic impedance, which is typically 50 Ω and corresponds to free space in optics. Therefore, a typical glass layer ($n = 1.5$) with thickness h_1 can, for example, be expressed as a 75 Ω impedance with phase delay $\delta_1/2$. (This analogy is valid when the conventional reflection coefficient $\Gamma_2 = (Z_2 - Z_1)/(Z_2 + Z_1) = (n_2 - n_1)/(n_2 + n_1)$ from medium 1 to 2 is used. If the other convention, as in Ref. 2, $\Gamma_2 = (Z_2 - Z_1)/(Z_2 + Z_1) = (Y_1 - Y_2)/(Y_1 + Y_2) = (n_1 - n_2)/(n_1 + n_2$, is adopted, all the expressions in the article would be modified by replacing the term impedance with admittance and altering the Smith charts accordingly.)

According to classical circuit theory for a cascaded network, the equivalent impedance at a given position can be readily obtained. Since reflection originates from impedance (index in optics) discontinuities at boundaries, an equivalent reflection at a specific position can be extracted from the corresponding mismatches.

For the single-layer case, the overall reflection is associated with the S-parameter at the front boundary $[S]^2$, as well as the reflection at the interior boundary at the back of the layer, Γ_1. This relation is also valid for the double layer case in which the total reflection at the foremost boundary, Γ_3, is obtained from $[S]^3$ and Γ_2.

For the multiple, N-layer case, the total reflection at the k_{th} boundary (Γ_k) is generalized with $[S]^k$ and Γ_{k-1}. As a result, the total reflection at the N-th layer is

$$R^{(N)} = \Gamma_{N+1} = S_{11}^{N+1} + \frac{S_{12}^{N+1} S_{21}^{N+1} \Gamma_N e^{i\delta_N}}{1 - S_{22}^{N+1} \Gamma_N e^{i\delta_N}}$$

where

$$\Gamma_N = S_{11}^N + \frac{S_{12}^N S_{21}^N \Gamma_{N-1} e^{i\delta_{N-1}}}{1 - S_{22}^N \Gamma_{N-1} e^{i\delta_{N-1}}}, \ldots, \; \Gamma_1 = S_{11}^1 \tag{3}$$

The transmission also has recursive characteristics associated with any previous equivalent transmission. However, the transmission at each layer also has to include the previous equivalent reflection term. This is because each transmission shares identical feedback terms that are described using the reflection.

The generalized transmission can be written as

$$T^{(N)} = T_1 = \frac{S_{21}^1 T_2 e^{i\frac{\delta_1}{2}}}{1 - S_{22}^2 \Gamma_1 e^{i\delta_1}}$$

$$\text{where} \quad T_2 = \frac{S_{21}^2 T_3 e^{i\frac{\delta_2}{2}}}{1 - S_{22}^3 \Gamma_2 e^{i\delta_2}}$$

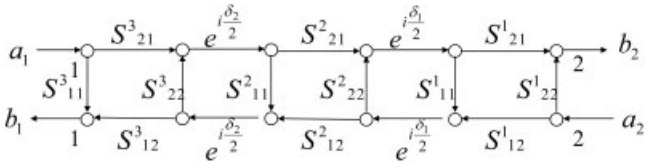

Figure 2 Signal flow graph of a double-layer structure

$$,\ldots,\ T_N = \frac{S^N_{21}T_{n+1}e^{i\frac{\delta_N}{2}}}{1 - S^{N+1}_{22}\Gamma_N e^{i\delta_N}},\ T_{N+1} = S^{N+1}_{21} \tag{4}$$

The superscripts on R and T indicate the number of layers. The expression using optical parameters can be obtained by simply replacing the S parameters using Eq. (1).

3. SIGNAL FLOW GRAPH APPROACH

Based on standard feedback theory, any arbitrary feedback network can be expressed conveniently with a signal-flow graph. An example for a double layer is given in Figure 2. Four basic topographical rules (branches in series, branches in parallel, elimination of self-loop, and node-splitting) are discussed by Dunn [7] for transforming such networks to a single path.

Such a transform is illustrated in Figure 3, where excluding the reflective paths in Figure 2 results in the transmission-flow graph of Figure 3(a). There is one forward transmission path ($S^3{}_{21}-S^2{}_{21}-S^1{}_{21}$) and three feedback-loop paths ($S^3{}_{22}-S^2{}_{11}$, $S^3{}_{22}-S^2{}_{21}-S^1{}_{11}-S^2{}_{12}$, $S^2{}_{22}-S^1{}_{11}$). A difficulty does arise due to the path containing the longest loop, $S^2{}_{12}$, but this can be eliminated by replacing $S^2{}_{11}$ and $S^I{}_{11}$ with Γ_2 and Γ_1. This technique discontinues the inter-relationship between the two layers, and thus

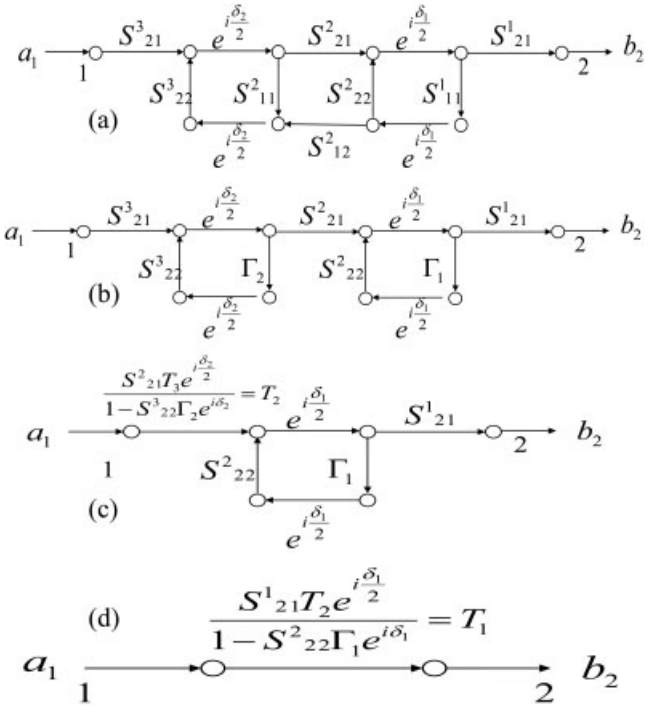

Figure 3 Topographical transform of a double-layer transmission to a single equivalent-signal-flow graph. (a) Transmission-flow graph of a double layer; (b) transform into two independent and equivalent layers; (c) elimination of the first independent feedback loop; (d) elimination of the second independent feedback loop

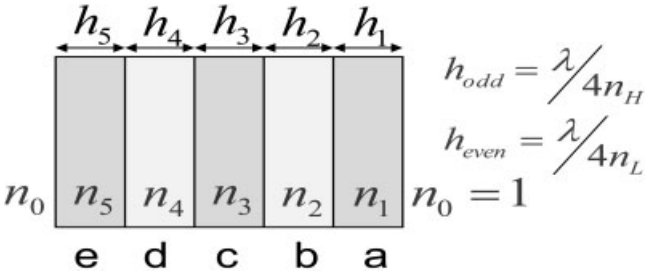

Figure 4 Five-layer optical system with quarter-wavelength layers of zinc sulfide and magnesium fluoride, labeled a–e

each single-layer loop becomes independent as illustrated in Figure 3(b). Likewise, the two single-layer loops can be transformed to one single-layer loop [Fig. 3(c)], and eventually, the double-layer transmission $T^{(2)}(=T_1)$ is reformulated in terms of equivalent, prior-layer transmissions in the identical format of Eq. (4) [Fig. 3(d)]. This provides a verification of the recursive pattern.

4. MICROWAVE APPROACH FOR OPTICAL THIN- FILM LAYERS

Symmetric, quarter-wave dielectric layers are a standard prototype for high-reflectors in the optical regime. The contribution of each quarter-wavelength layer to a five layer reflector is analyzed here using a recursion formula. A graphical interpretation using microwave methods is also presented to demonstrate the ease of isolating each layer's contribution to the system's reflectance.

Although graphical techniques for optical multilayer systems that assist conceptual design have been reported, e.g., by Apfel [9], the standard graphical tool for microwave engineering—the Smith chart—can be utilized to visualize optical design in a similar fashion. In microwave design, one of the primary goals is to maximize power flow by minimizing impedance mismatches, and the Smith chart has been a valuable tool to visualize the control of reflections. This impedance-reflection conversion as a function of microwave frequency is the essence of the Smith chart, and it can also be applied to the index-reflection conversion as a function of optical wavelength.

For example, a five-layer, quarter-wavelength optical system consisting alternately of zinc sulfide ($n_{\text{odd}} = n_H = 2.3$) and magnesium fluoride ($n_{\text{even}} = n_L = 1.35$), as shown in Figure 4, gives a power reflectance ($|\Gamma|^2$) of 0.9141. This value decreases to 0.7704 for a three-layer system (layers cba only in Fig. 4) and 0.4652 for a single layer (a only).

The graphical explanation of this quarter-wave reflector is presented in Figure 5(a). Each layer makes a circular trace that starts from the equivalent reflection point from the previous layer. The radius of this trace is determined by the index of the corresponding layer. The circles are periodic with every half wavelength. This means the quarter-wavelength layers form semicircles that push their traces toward the unity boundary in a spiral pattern. This spiral is achieved by alternating quarter- wave layers of high and low index material, and it approaches the unity circle as the number of layers increases. The dashed circle represents the final reflection after the fifth layer, e. The circle originates at the center (50 Ω point) and yields the same reflection with different phases.

Reflection traces for each of the five layers of the coating for a broad wavelength band are given in Figure 5(b). Reflections at the λ_0 line also seen in Figure 5(b), which explains why $\Gamma_b < \Gamma_a$, $\Gamma_d < \Gamma_c$. When the number of quarter-wave layers increases, the reflection is observed to be higher, but the reflection bandwidth is shown to decrease, as expected. The reason for this is that fewer

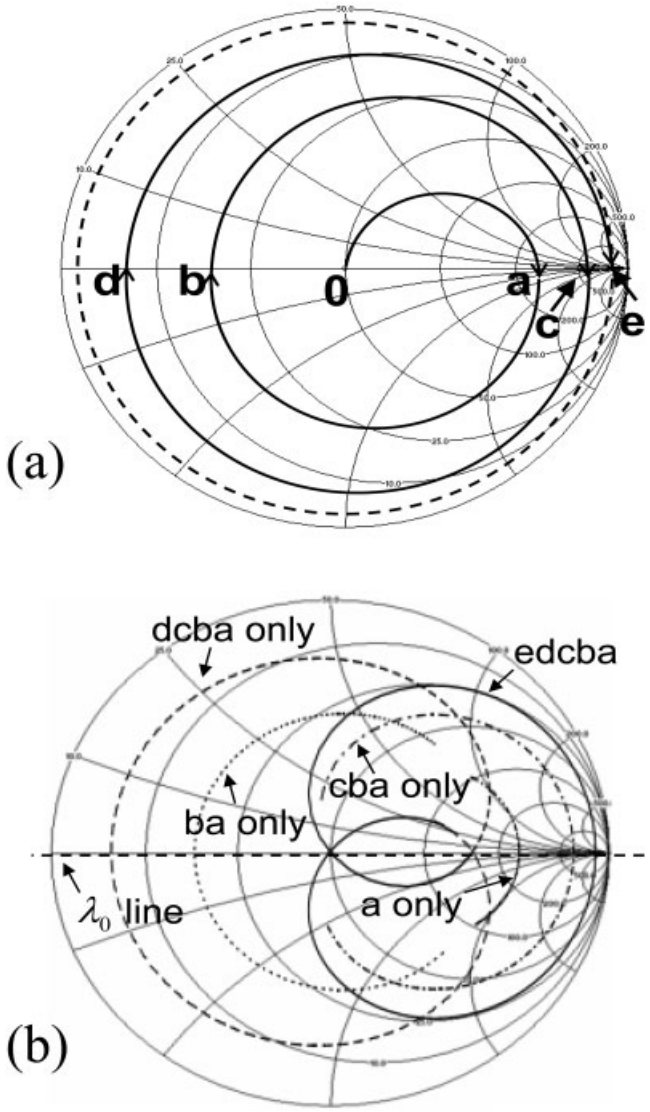

Figure 5 (a) Evolution of optical reflection on a Smith chart for a cumulative quarter wavelength multiple stack of five elements at λ_0. (b) Individual reflections on Smith chart for a cumulative quarter wavelength multiple stack of five elements, vs. wavelength (or frequency) (0.7 λ_0 [le] λ [le] 1.7 λ_0)

wavelengths can adequately satisfy the quarter-wavelength condition as the number of spiral turns increases. The use of the Smith chart thus offers excellent design advantages. For instance, the graphical transition of the reflection trace with additional layers can be easily predicted based on the index and thickness of a layer.

The reflection at a specific frequency can be readily moved to other points simply by adding layers with appropriate parameters. Each additional layer gives an inscribed circle with a half-wavelength period. A larger refractive index results in a smaller diameter. This is fundamentally the same as series stub tuning in microwave theory. Unfortunately, parallel stub tuning cannot be realized in optics because the reactive part of the refractive index in dielectric materials is typically negligible and difficult to manipulate. This graphical tuning method allows a designer to observe the tuning range of single additional layers with a given index of refraction. This also determines the number of layers necessary to reach the final tuning objective.

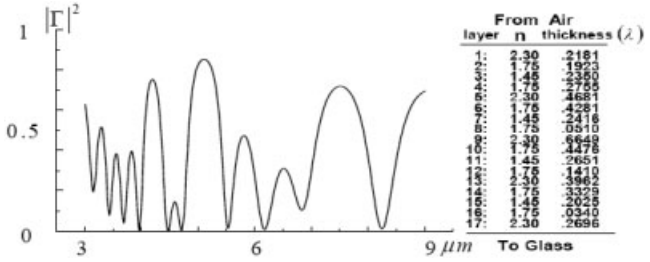

Figure 6 Power reflectance vs. wavelength for a 17-layer reflector designed for a 5-μm wavelength [10] [using the recursion expression in Eq. (3)]

5. PRACTICAL MULTILAYER ANALYSES

To evaluate the recursion formula presented in Eq. (4), we have chosen the example of a practical, 17-layer mid- infrared reflector. The example optical reflector was designed to have a maximum reflectance at a wavelength of 5 μm with zero reflectance at 4.5 μm and 5.5 μm. This specification was achieved by an optimization method using layer perturbation in a computation-intensive Monte Carlo approach [10].

Given the refractive index and the thickness in terms of wavelength for each layer, the power reflectance is also computed using the expressions in Eq. (3). Figure 6 shows the results from the recursion analysis; they are observed to be identical to those of the conventional method. The specified design spec in Ref. 10 (85% reflection at 5 μm center wavelength with a 1 μm null bandwidth) was realized using a diverse set of 17 asymmetric optical layers. This optical design simulation was reproduced using purely the microwave and feedback approaches.

The microwave approach for a multilayer system may best be suited for the THz region - the underutilized band between the microwave and infrared portions of the spectrum. Thus, a computational example for a THz mirror previously designed with a transfer-function method is chosen [11] for comparison with the recursion analysis. The mirror consists of 25 ceramic layers of a Bragg-grating stack to be used with a broadband THz source, such as those that employ ultrafast lasers in the generation of a signal. Since the THz generator was an optical-based source, the simulation of the reflection performance was compared in Ref. 11 to the experiment using a purely optical approach. Power-transmittance results across the THz spectral range, computed using the recursion methodology developed herein, are shown in Figure 7. A wide high reflectance region that matches that from the previous design [11] is observed.

6. CONCLUSIONS

Optical multilayers were analyzed from the perspective of both microwave and feedback theory. Transmission and reflection co-

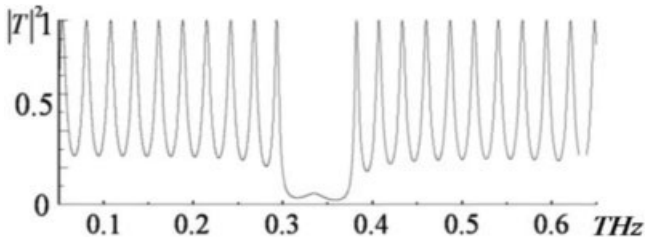

Figure 7 Power transmittance of a practical 25-layer reflector for wideband THz beams [suggested in Ref [11]. (n_{odd} = 3.17, n_{even} = 4.16, h_{odd} = 73 μm, h_{even} = 51 μm), computed with the recursion formula (4)

efficients were replaced with more general expressions that utilized microwave *S*-parameters. As *S*-parameters can handle a frequency-dependent gain medium, this novel approach is useful for even active optical-feedback systems such as laser cavities. It was shown that the signal flow graph approach, also a powerful technique, can be extended to parallel-coupled systems such as interferometers. The analysis using a nonmatrix approach was not only simple, but also visually advantageous for design.

REFERENCES

1. R. Guenther, Modern optics, Chapter 3, Wiley, New York, NY, 1990.
2. L. Young, Synthesis of multiple antireflection films over a prescribed frequency band, J Opt Soc Am 51 (1961), 967–974.
3. L. Young and E.G. Cristal, Low~pass and High~pass filters consisting of multilayer dielectric stacks, IEEE Trans Microwave Theory Tech 48 (1966), 75–80.
4. P. Baumeister, Application of microwave technology to design an optical multilayer bandpass filter, Appl Opt 42 (2003), 2407–2414.
5. S.J. Mason, Feedback theory Some properties of signal flow graphs, Proc IRE 41 (1953), 1144–1156; 44 (1956), 920–926.
6. G. Gonzalez, Microwave transistor amplifiers analysis and design, Chapter 2, Prentice Hall, New Jersey, 1997.
7. M.H. Dunn, Use of flow graphs in the analysis of optical cavities, Appl Opt 10 (1971), 1393–1397.
8. D. Minkov, Flow-graph approach for optical analysis of planar structures, Appl Opt 33 (1994), 7698–7703.
9. J.H. Apfel, Graphics in optical coating design, Appl Opt 11 (1972), 1303–1312.
10. W.J. Wild and H. Buhay, Thin-film multilayer design optimization using a Monte Carlo approach, Opt Lett 11 (1986), n745–n747.
11. F. Rutz, M. Koch, L. Micele, and G. de Portu, Ceramic dielectric mirrors for the terahertz range, Appl Opt 45 (2006), 8070–8073.

IMPROVED PHASE NOISE FOR DIELECTRIC RESONATORS OSCILLATORS WITH BROADBAND TUNING

Liang Zhou[1] and Zhuo Wu[2]

[1] Center for Microwave and RF Technology, School of Electronic Information and Electrical Engineering, Shanghai Jiao Tong University, No. 800, DongChuan Road, Minhang District, Shanghai 200240, People's Republic of China; Corresponding author: liangzhou@sjtu.edu.cn

[2] Department of Communication Engineering, School of Communication and Information Engineering, Shanghai University, P.O.Box 160, No.149, Yanchang Road, Shanghai 200072, People's Republic of China

Received 8 September 2008

ABSTRACT: *In this article, we describe a method of design of very low phase noise dielectric resonators oscillators at 13 GHz. By using two Silicon Germanium transistors with total gains 8 dB and lower flicker noise corner between 10 kHz and 40 kHz, the phase noise of the oscillators can be achieved −125 dBc/Hz at 10 kHz offset. The resonator has unloaded Q around 14,000 at operating frequency and is then optimized and coupled to the amplifiers for minimum phase noise where* $Q_L/Q_0 = 1/2$ *hence* $S_{21} = -6$ *dB. To incorporate tuning, phase shifter is also investigated. The phase noise measurement system is also presented using two identical oscillators phase locked at the same frequency*. © 2009 Wiley Periodicals, Inc. Microwave Opt Technol Lett 51: 1312–1316, 2009; Published online in Wiley InterScience (www.interscience.wiley.com). DOI 10.1002/mop.24334

Key words: *DROs; phase noise; tuning; SiGe; flicker noise*

1. INTRODUCTION

Dielectric resonators oscillators (DROs) have a very good performance in the frequency stability, which could be distinction into short term stability and long term stability. The short term stability related with amplitude noise, phase noise, and jitter at oscillating frequency, whereas the long term stability considers frequency drift, which describe the variation of the frequency at long period of time.

Today's research for the DROs is focused on the high stability and very low phase noise, based on linear and nonlinear oscillator models. Ivanov and Tobar [1] demonstrated a low phase noise −160 dBc/Hz at 1 kHz offset for 9 GHz DROs using interferometric signal processing methods, Llopis et al. [2] presented an oscillator with phase noise −133 dBc/Hz at 1 kHz offset. Graval and Wight [3] described a 12 GHz push-push phase locked DROs with a phase noise −105 dBc/Hz at 10 kHz offset. Those DROs are used different unloaded quality factor sapphire resonators from 290,000 to 1,000,000 with Silicon Germanium HBT transistors due to lower flicker noise than GaAs and FETs. Based on the Leeson's oscillators model [4], the oscillators normally require a high unloaded Q resonator and an amplifier with high output power and lower flicker noise corner. The best room temperature oscillators currently available typically use sapphire resonators with sophisticated flicker noise reduction methods. However, there is a disadvantage of sapphire resonators at room temperature because of the large temperature coefficient. Therefore, those oscillators need very complex temperature compensation.

This article describes the design of very low phase noise dielectric resonators oscillators at 13 GHz including low noise amplifier, resonator, phase shifter and directional coupler. It will be shown that the phase noise is around −95 dBc/Hz at 1 kHz offset and −125 dBc/Hz at 10 kHz offset. A phase noise measurement system is also included to measure the performance of the DROs. The phase noise of these DROs is around 15 to 25 dB better than most commercial design at room temperature.

2. OSCILLATOR DESIGNS

The oscillator design is based on the use of an oscillator arranged in a positive feedback configuration consisting of Silicon Germanium amplifiers, an output coupler, varactor diode based phase shifter and high Q ceramic resonator as shown in Figure 1.

3. PHASE NOISE THEORY

Developing a simple and general model to calculate and predict the phase noise performance of an oscillator is important. A

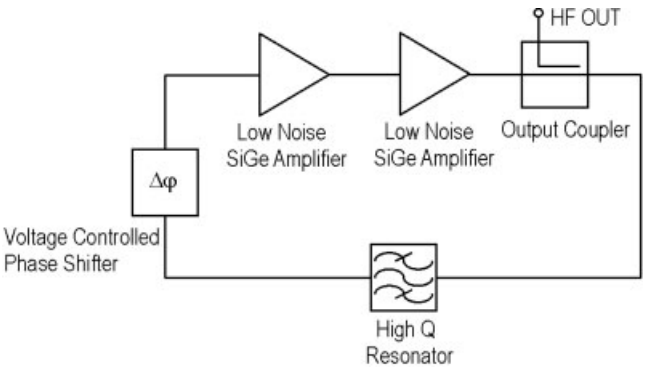

Figure 1 Oscillators configuration